Electronic Supporting Information

High-throughput robotic colourimetric titrations using computer vision

Contents

0 Chemicals.....4

1 The brief introduction of method and labware 4

1.1 The selection of chemical titration for high-throughput (HTE) H_2O_2 determination 4
1.2 The numbering rule of the labware 5
2 Protocol development 5
2.1 Development of system/transfer configuration 5
2.2 Development of pre-estimation in transfer configuration 6
2.3 Development of mixing in transfer configuration 6
2.4 Development of titration in transfer configuration 7
3 System/Transfer configuration 7
3.1 A brief introduction to system/transfer configuration 7
3.2 The calculation details of pre-estimation and titration 8
4 The Lab hardware for high-throughput H_2O_2 determination 9
4.1 The installation of webcam and light environment control 9
4.2 The interactive working system 10
5 Signal processing 11
5.1 Instance segmentation 11
5.2 Plate preparation/Pre-estimation image analysis 12
5.3 Fitting analysis in titration 12
6 The schematic diagram of this workstation 15
6.1 The schematic diagram of this workstation 15
6.2 Software & Packages used in this workstation 15
7 Evaluation 15
7.1 Sensitivity test 15
7.2 Precision test 17
7.3 Linear dynamic range 18
7.4 Accuracy test 18
7.5 The operation time 20
7.6 The scalability test 21
8 Application 22
8.1 Monitoring H_2O_2 production through photocatalysis 22

8.2 Parameter Selection 22

8.3 The acidity/alkalinity test.....23

8.4 Water hardness analysis (Calcium Analysis by EDTA titration) 24

References 26

0 Chemicals

Table S1 Chemicals

Chemical	Purity	Company	Post-treatment
H_2O_2 determination (Redox titration)			

Potassium permanganate solution	standardised against sodium thiosulfate c($KMnO_4$) = 0.02 mol/L (0.1 N) Titripur® Reag. Ph Eur	Sigma Aldrich	NA
Hydrogen peroxide solution	3 wt.% in water, contains stabilizer	Sigma Aldrich	NA
Sulfuric acid	98%	Sigma Aldrich	NA
Potassium iodide	99.9% metals basis	Thermo Fischer	NA
Potassium hydrogen phthalate	primary standard	Alfa Aesar	NA
Acid-Base titration			
Sodium hydroxide	Analytical reagent grade	Fischer Chemical	NA
Hydrochloric acid	Analytical reagent grade	Fischer Chemical	NA
Methylene orange	>99.5%	Fluorochem	NA
Water Hardness Analysis (Complexometric Titration)			
Calcium carbonate	Laboratory reagent grade	Thermo Fischer	Dry at oven at 60 ℃ for 2 hours
Magnesium chloride	≥ 98%, anhydrous	Fluorochem	NA
Hydrochloric acid	Analytical reagent grade	Fischer Chemical	NA
Eriochrome black T (EBT)	ACS Reagent (indicator grade)	Sigma Aldrich	NA
Ethylenediaminetetraacetic acid (EDTA) disodium salt dihydrate	≤0.005% Insolubles ≤0.1% Nitrilotriacetic acid (NTA) Fe: ≤0.005%, Pb: ≤0.002%	Sigma Aldrich	NA
Ammonium chloride-ammonium hydroxide buffer solution, in H_2O	pH=10-11	Sigma Aldrich	NA

1 The brief introduction of method and labware

1.1 The selection of chemical titration for high-throughput (HTE) H_2O_2 determination

For titration methods used for HTE H_2O_2 determination, titration combined with spectrophotometry and fluorometry leverages high extinction coefficients and enables estimation at the micro-molar level[1], but their complex operations and long reaction time limit their application in automation. In contrast, chemical titration using $KMnO_4$ is suitable for HTE H_2O_2 determination, which can measure H_2O_2 from medium to high concentrations, at a maximum of 30 mM. For this chemical reaction as shown in Equ. 1, MnO_4^-, possessing a purple colour, is reduced into colourless Mn^{2+} by H_2O_2. Once excess $KMnO_4$ is added to this system, a pale pink colour will appear. The titration endpoint is reached when this pale pink colour lasts for 30 seconds, which could be monitored by the camera and further analysed by colourimetry, a science for quantify colour information.

$$2KMnO_4^- \text{ (purple)} + 6H^+ + 5H_2O_2 \rightarrow 2Mn^{2+} + 8H_2O + 5O_2\uparrow \text{ (Equ. 1)}$$

1.2 The numbering rule of the labware

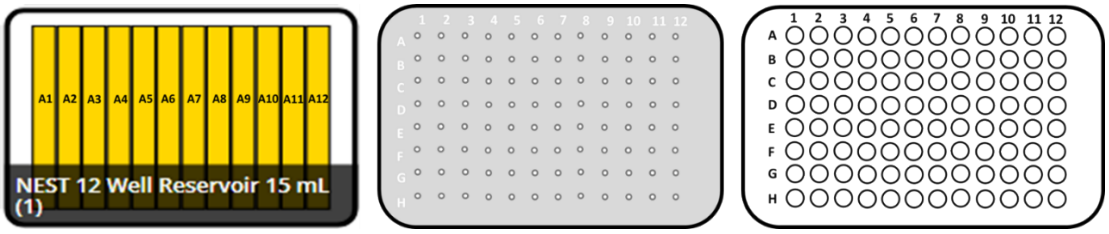

Figure S1 The layout and numbering rule of the reservoir, tip rack, and white 96-well flat-bottom plate.

2 Protocol development

The protocol designer script was divided into system configuration and transfer configuration setups: (1) The system configuration defined the labware and robot configuration. For example, using Corning's 96-well plate for titration required setting the labware name, deck position and labware offset, if any. We used Azenta's 12-well reservoir for $KMnO_4$ storage and Corning's 96-deep well reservoir for H_2O_2 storage. These definitions were used by OT-2 to map the corresponding calibrated dimensions for correct manoeuvring. Robot configurations consisted of pipette assembly (P300 Gen2 and P20 Gen2) and pipette parameters; (2) The transfer config tasks were split into the following parts: plate preparation (H_2SO_4 and H_2O_2 transfer), pre-estimation, and titration.

2.1 Development of system/transfer configuration

Unlike the traditional chemical titration of H_2O_2 using $KMnO_4$, no matter what type of plate was chosen for automation, its volume is quite limited (200 ~ 2000 µL, data from Opentrons' official website). Thus, the concentration range of H_2O_2 and corresponding $KMnO_4$ used for titration needed to be confirmed. A literature review was carried out to confirm the highest amount of H_2O_2 produced by photocatalysts without using a sacrificial agent. Up to now, the highest reported H_2O_2 concentration produced by CoO_x/Mo:$BiVO_4$/Pd is ~7 mM[2]. Initially, 0~10 mM was chosen as the targeted concentration range to develop this high-throughput H_2O_2 determination.

Based on these, details (like the type of the plate, the volume of the H_2O_2, the volume and concentrations of H_2SO_4, and the corresponding volume of $KMnO_4$) were further confirmed. Considering the influence of the depth of the well on the observation of the colour change in each well and the requirements to develop automation, a frequently used 96-well plate with a total volume of 360 µL was chosen as the reaction container to complete the titration as the traditional chemical titration. For the 96-well plate, it had three colour options, including transparent, white, and black. Among them, the transparent plate was used for optical or colorimetric experiments. The black plate was recommended for fluorescence measurements due to its minimal backscatter and low background fluorescence. The white plate, on the other hand, was widely used in luminescence measurements because of their maximum reflection, minimal crosstalk between the wells and low autoluminescence[3]. Given that the colour change of the titration endpoint was quite subtle, from transparent to pale pink. Thus, to better capture the slight colour change, a white plate was selected to strengthen this colour change and minimize crosstalk between different wells. After considering the volume range (20~300 µL) of the multi-channel pipette currently attached to the OT-2, experimental accuracy, and the volume effect, each column of the plate was finally charged with 100 µL H_2O_2 of the same concentration (0~10 mM) and 100 µL 1 M H_2SO_4. In these trials, the concentration of H_2O_2 was known to chemists so that they could choose a suitable concentration of $KMnO_4$ to achieve the titration within the limited volume. However, when it comed to the robot to operate this colorimetric titration experiment without an estimation of titrant range, it was difficult for robot to select an appropriate $KMnO_4$ titrant solution for H_2O_2 determination. For example, at equivalence point, 100 µL 1 mM & 10 mM H_2O_2 consumed 40 µL & 400 µL of 1 mM $KMnO_4$, respectively, thus causing liquid overflow if a typical 96-well plate was used. Therefore, an extra pre-estimation was created before the final titration to solve this problem.

2.2 Development of pre-estimation in transfer configuration

The design of the pre-estimation referred to the 'conditional statements' in programming, which is crucial for controlling the flow of a program and implementing logic that responds to varying inputs or situations.

The H_2O_2 concentration was initially divided into four ranges. And then, based on stoichiometric ratio of the redox reaction, the total 360 μL volume of each well and the convenience of automation, athe concentration of $KMnO_4$ was adjusted. The results were summarised in Table S2.

Table S2 The calculation details of the pre-estimation

H_2O_2 concentration (mM)	**$KMnO_4$ Concentration (mM)**	**Consumed $KMnO_4$ volume (μL)**
0-1	1	0-40
1-2	2	20-40
2-4	4	20-40
4-10	10	16-40

**H_2O_2 volume: 100 μL; H_2SO_4: 1 M, 100 μL.*

As shown in Table S2, the maximum consumed $KMnO_4$ volume of each concentration range of H_2O_2 was 40 μL. If 100 μL H_2O_2 sample with an unknown concentration reacted with 40 μL of four different concentrations of $KMnO_4$ respectively, there must be at least one case where the solution showed some colour varying from pale pink to purple. In each column of the plate, rows of 5-8 (or E-H) were selected for pre-estimation and charged with 40 μL 1 mM, 2mM, 4mM, and 10mM $KMnO_4$ concentration, respectively. Then, the mixture was mixed manually by a pipette with a volume range of 10-100 μL and its result was displayed in Figure S2.

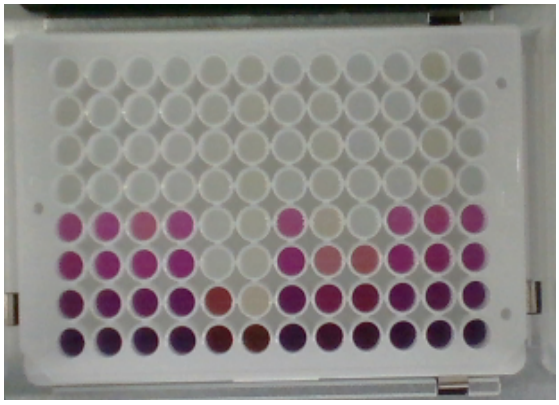

Figure S2 The pre-estimation image of a 96-well plate captured by the webcam (manual experiment).

2.3 Development of mixing in transfer configuration

When verifying the feasibility of the pre-estimation stage using the robot OT-2, we found that all wells located in rows E-H of each column showed a colour from pale pink to purple, no matter how high the H_2O_2 concentration was. This was because a single-channel pipette was utilized to only add $KMnO_4$ in rows E-H and its maximum volume was only 20 μL, quite smaller than the existing solution (200μL) in the well. Therefore, the diffuse effect was observed in the pre-estimation. To overcome this issue, an extra step, mixing solution using the multi-channel pipette with a maximum volume of 300 μL, was added after aspirating $KMnO_4$ solution each time. The mixing volume was set as 100 μL and repeated 5 times. Also, to be economical and environmentally friendly, an extra water reservoir was added to rinse tips after mixing, which could reduce the consumption of tips and diminish the influence of the

remaining solution in tips. However, even though this step could highly increase the accuracy of the result, this step correspondingly increased the operation time.

2.4 Development of titration in transfer configuration

For the titration stage, the maximum volume of consumed $KMnO_4$ was 40 μL as shown in Table S2. However, it is hard to gain the titration endpoint for the highest H_2O_2 concentration in each range with only one point on the equilibrium. To overcome this issue, the total $KMnO_4$ volume used for titration was set as 60 μL. As discussed in the development of pre-estimation, rows E-H in each column have been selected for the pre-estimation. To minimize random error, rows A-D were chosen for titration, which could allow each sample to be measured four times in parallel. But until now, the volume of each step has not been confirmed, which is quite important for the following signal processing and fitting analysis. The lower the volume of each step, the more operation time was required, even though it can produce more points for fitting analysis. During the titration experiment, the solution was transparent until a stoichiometric equilibrium was reached, which could be fitted by a straight line. In addition, the minimum volume of consumed $KMnO_4$ was mostly ~20 μL except for 0-1 mM H_2O_2 concentration range as displayed in Table S2. To obtain enough points for the linear fitting in the piecewise fitting and save operation time, 5 μL was set to one step and repeated 12 times.

3 System/Transfer configuration

```
In [2]: from setting.setting_h2o2 import *

System Config

In [ ]: sh = system_config_h2o2()

sh.dict['tiprack_1']['type'] = 'opentrons_96_tiprack_20ul'
sh.dict['tiprack_2']['type'] = 'opentrons_96_tiprack_20ul'
sh.dict['tiprack_3']['type'] = 'opentrons_96_tiprack_300ul'
sh.dict['tiprack_4']['type'] = 'opentrons_96_tiprack_300ul'
sh.dict['tiprack_1']['pos'] = 10 # for titration
sh.dict['tiprack_2']['pos'] = 11 # for titration and pre-estimation
sh.dict['tiprack_3']['pos'] = 1 # for samples(h2o2)
sh.dict['tiprack_4']['pos'] = 8 # for buffer(h2so4) and indicator
sh.dict['reservoir_1']['pos'] = 9 # samples(h2o2) reservoir
sh.dict['reservoir_2']['pos'] = 6 # buffer(h2so4) and indicator reservoir
sh.dict['reservoir_3']['pos'] = 7 # titrant(KMno4) reservoir
sh.dict['reservoir_4']['pos'] = 4 # h2o reservoir
sh.dict['tiprack_1']['offset']['x'] = 0.10
sh.dict['tiprack_1']['offset']['y'] = 0.30
sh.dict['tiprack_1']['offset']['z'] = 0.20
sh.dict['tiprack_2']['offset']['x'] = 0.50
sh.dict['tiprack_2']['offset']['y'] = 0.20
sh.dict['tiprack_2']['offset']['z'] = 0.30
sh.dict['tiprack_3']['offset']['x'] = -0.70
sh.dict['tiprack_3']['offset']['y'] = 0.7
sh.dict['tiprack_3']['offset']['z'] = 0.10
sh.dict['tiprack_4']['offset']['x'] = -0.20
sh.dict['tiprack_4']['offset']['y'] = 0.90
sh.dict['tiprack_4']['offset']['z'] = 0.00
sh.dict['plate_1']['offset']['x'] = -0.10
sh.dict['plate_1']['offset']['y'] = 0.20
sh.dict['plate_1']['offset']['z'] = 0.80
sh.dict['pipette_1']['type'] = 'p300_multi_gen2'
sh.dict['pipette_1']['mount']='left'
sh.dict['pipette_2']['type'] = 'p20_single_gen2'
sh.dict['pipette_2']['mount']='right'
sh.save_json()
```

```
In [ ]: tc = transfer_config_h2o2()
# Note: volume number must be between the minimum and the maximum range of the u
# Transfer 1 : Buffer or Indicator addition(H2SO4), Multi-Channel Pipette p300,
tc.dict['transfer_1']['tiprack'] = ['A1:A12']
tc.dict['transfer_1']['vol'] = {'A1':100} # volume aspirate uL
tc.dict['transfer_1']['locs'] = [['A1','A9:A10']] # buffer + indicator in all co
tc.dict['transfer_1']['blowout'] = True
tc.dict['transfer_1']['mix'] = None


# Transfer 2 : Sample Addition(H2O2), Multi-Channel Pipette p300, tiprack_3
tc.dict['transfer_2']['tiprack'] = ['A1:A12']
tc.dict['transfer_2']['vol'] = 100 # volume aspirate uL
tc.dict['transfer_2']['locs'] = ['A1:A2','A9:A10']
tc.dict['transfer_2']['blowout'] = True
tc.dict['transfer_2']['mix'] = None


# Transfer 3 : Pre-estimation(titrant), Single-Channel Pipette p20, tiprack_2: E
# Note: the input volume is 20 uL, but within the titration_general.py, this asp
# 40 uL in total for each concentration of titrant
# select the condition parameter, including a_star and hue (hue_threshold and di
tc.dict['transfer_3']['tiprack'] = ['E11:H11']
tc.dict['transfer_3']['vol'] = 20 # volume aspirate uL
tc.dict['transfer_3']['locs'] = [['A1','E9:E10'],
                                 ['A2','F9:F10'],
                                 ['A3','G9:G10'],
                                 ['A4','H9:H10']]
tc.dict['transfer_3']['mix'] = {'rep' : 0, 'vol' : 20}
tc.dict['transfer_3']['blowout'] = True
#tc.dict['transfer_3']['param'] = 'a*'
tc.dict['transfer_3']['params'] = 'hue'
tc.dict['transfer_3']['boundary'] = 2  # Threshold used to identify the titratio
tc.dict['transfer_3']['larger_than_boundary'] = False # Boolean(type) indicating


# Transfer 4 : Titration(titrant), Single-Channel Pipette p20, tiprack_1
tc.dict['transfer_4']['tiprack'] = ['A1:H12','A1:H12']
tc.dict['transfer_4']['vol'] = 4 # volume aspirate uL
tc.dict['transfer_4']['locs'] = [['A3','A4'],['A9:A10'] ]
tc.dict['transfer_4']['titration'] = [15] * len(tc.dict['transfer_4']['locs'][0]
tc.dict['transfer_4']['mix']['rep'] = 0
tc.dict['transfer_4']['mix']['vol'] = 20
tc.dict['transfer_4']['blowout'] = True
tc.dict['transfer_4']['speed'] = {'aspirate' : 1, 'dispense' : 1}
tc.save_json()
tc
```

Figure S3 The system/transfer configuration defined in 'Protocol_setup_h2o2.ipynb'.

3.1 A brief introduction to system/transfer configuration

System/transfer configuration was defined in 'Protocol_setup_H2O2.ipynb'.

(1) The labware configuration in 'system config':

sh = system_config_h2o2() -- create an instance from class system_config_h2o2, containing the basic information

sh.dict['tiprack_1']['type'] = 'opentrons_96_tiprack_20ul' -- define the type of the labware

sh.dict['tiprack_1']['pos'] =10 -- define the position of the labware

sh.dict['tiprack_1']['offset']['x'] = 0.10 -- define the offset alignment of the labware

(2) The robot configuration in 'system config':

sh.dict['pipette_1']['type'] = 'p300_multi_gen2'

sh.dict['pipette_1']['mount']='left'

Robot configurations consist of pipette assembly (P300 Gen2 and P20 Gen2) and pipette parameters. All these offset alignments are obtained after running the H_2O_2 offset alignment protocol in the Opentrons software in the set-up stage. After inputting these essential data, use the command *sh.save_json()* to save and transfer it to shared folder of SMB server.

(3) The liquid transfer instructions defined in 'transfer config':

The 'transfer_config' contains the liquid transfer rules, including plate preparation (sulfuric acid addition and H_2O_2 addition), pre-estimation, and titration. The deck information and labware information will be taken from 'system_config' and parsed inside run_opentron (pi) through SMB server. Meanwhile, to further improve the universality of our transfer configuration, it could be generally classified into plate preparation, including transfer_1 and transfer_2 for addition of buffer/indicator and sample, pre-estimation (transfer_3) for and titration (transfer_4). All these details for system/transfer configuration could be found in Figure S3. To extend this workstation to other titration chemistries, three parameters (*params*, *boundary*, and *larger_than_boundary*) were added to transfer_3.

3.2 The calculation details of pre-estimation and titration

Table S3 The calculation details of the added volume of the $KMnO_4$ solution

$KMnO_4$ Conc.	H_2O_2 Conc./ mM	H_2O_2 Volume/μL	1 M H_2SO_4 Volume/μL	$KMnO_4$ Cal. Volume/μL
A4	10	100	100	40
A4	9.5	100	100	38
A4	9	100	100	36
A4	8.5	100	100	34
A4	8	100	100	32
A4	7.5	100	100	30
A4	7	100	100	28
A4	6.5	100	100	26
A4	6	100	100	24
A4	5.5	100	100	22
A4	5	100	100	20
A4	4.5	100	100	18
A4	4	100	100	16
A3	4	100	100	40
A3	3	100	100	30
A3	2.5	100	100	25
A3	2	100	100	20
A2	2	100	100	40
A2	1.5	100	100	30
A2	1	100	100	20
A1	1	100	100	40
A1	0.8	100	100	32
A1	0.6	100	100	24
A1	0.4	100	100	16

A1	0.2	100	100	8
A1	0.1	100	100	4

*A1: 1 mM; A2: 2 mM; A3: 4 mM; A4: 10 mM.

4 The Lab hardware for high-throughput H_2O_2 determination

4.1 The installation of webcam and light environment control

To achieve in-situ colour analysis, a webcam (Intel RealSense Depth Camera D435i) was fastened to the pipette mount of the OT-2 using a screw, which could allow the camera to easily move and further gain a best view of the target plate in deck 5 as shown in Figure S4.

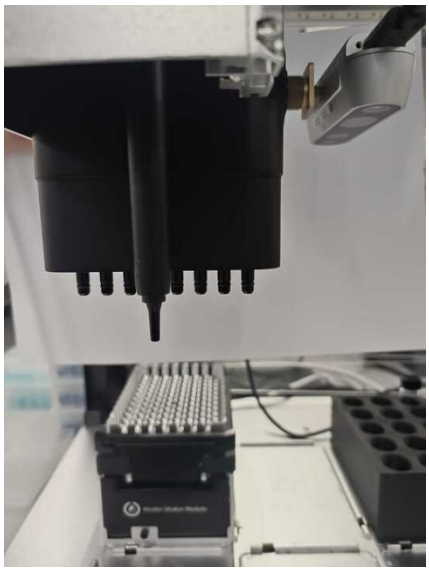

Figure S4 The Intel RealSense Depth Camera D435i on the pipette mount.

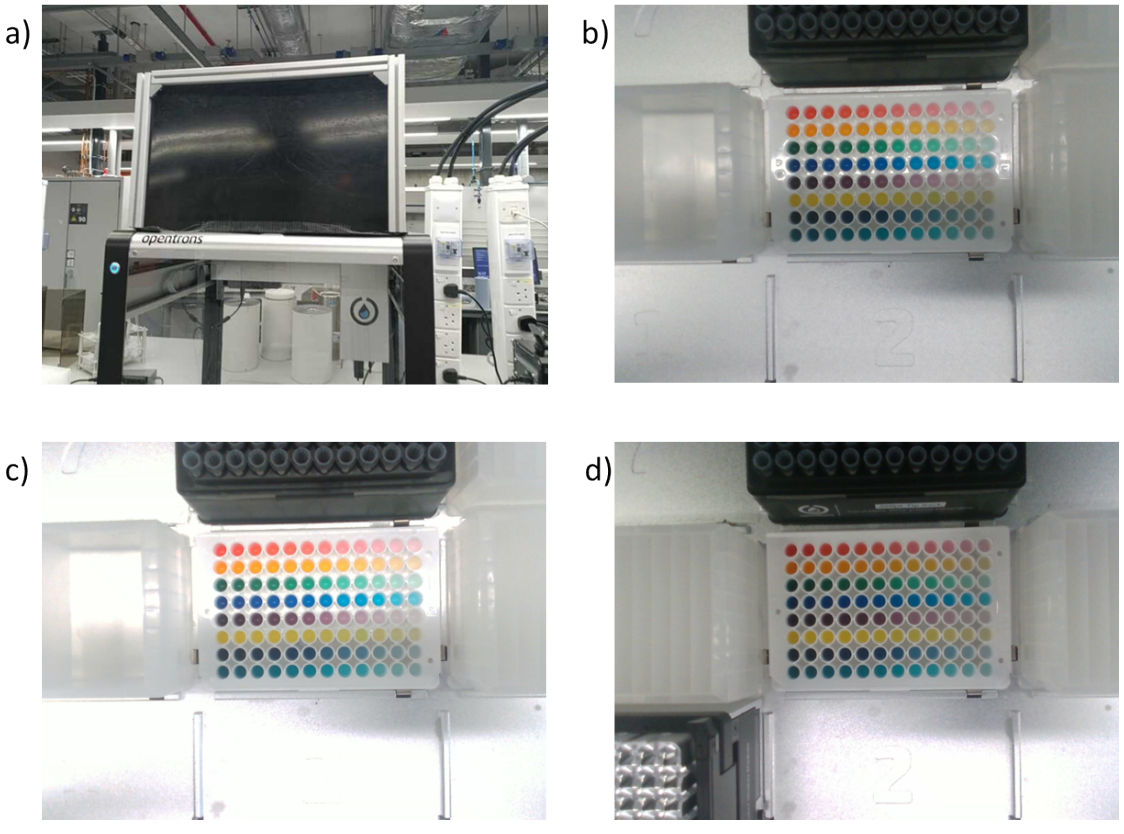

Figure S5 a) The black box installed on the top of the Opentrons platform for light control; b, c) Images taken without the black box at camera sensitivities of b) 110 and c) 111; d) image taken with the black box at a sensitivity of 11, showing fewer reflections and better lighting uniformity

To enhance the reliability of the computer vision technique, illumination conditions were controlled. Specifically, to mitigate light effects during experiments, a custom black box was constructed to replace the top panel of the Opentrons platform, and the built-in light source was turned off. (Figure S5(a)). Two images taken without the black box at different sensitivity settings revealed significant impacts from the reflected light, including overexposure and shadows cast by the OT-2 gantry, as shown in Figure S5(b, c). In contrast, in Figure S5(d), the image captured with the black box, even at high sensitivity, exhibited superior quality with reduced glare and more consistent illumination.

4.2 The interactive working system

In this working system, a service message block (SMB) server was chosen to combine OT-2 with our working PC. In detail, Opentron provided both graphical & python scripting for developing a protocol. The graphical interface created necessary labware definition & liquid transfers by embedding commands in an instruction file (JSON format), whereas the Python scripting leveraged Opentron's Python library. To execute the commands, the instruction file or Python script needed to be uploaded to the OT-2 app. As described before, titration protocol development required titrating H_2O_2 with $KMnO_4$ and subsequent image capture, thus requiring synchronization of the OT-2 robot with an imaging system, which was impossible if the OT-2 app was used. The Python scripting also provided a scope to communicate directly to the OT-2's Raspberry Pi and this further facilitated synchronization with our imaging system. We set up an SMB server in our local PC that was visible to the Raspberry Pi (remote). By continuously monitoring appropriate file addition or upgradation to SMB server, the local PC & Raspberry Pi can perform the necessary task. For example, when we add 5 µL of $KMnO_4$ to H_2O_2, Raspberry Pi sent a trigger to the SMB server which further prompted the local PC to activate the camera and capture an image.

5 Signal processing

5.1 Instance segmentation

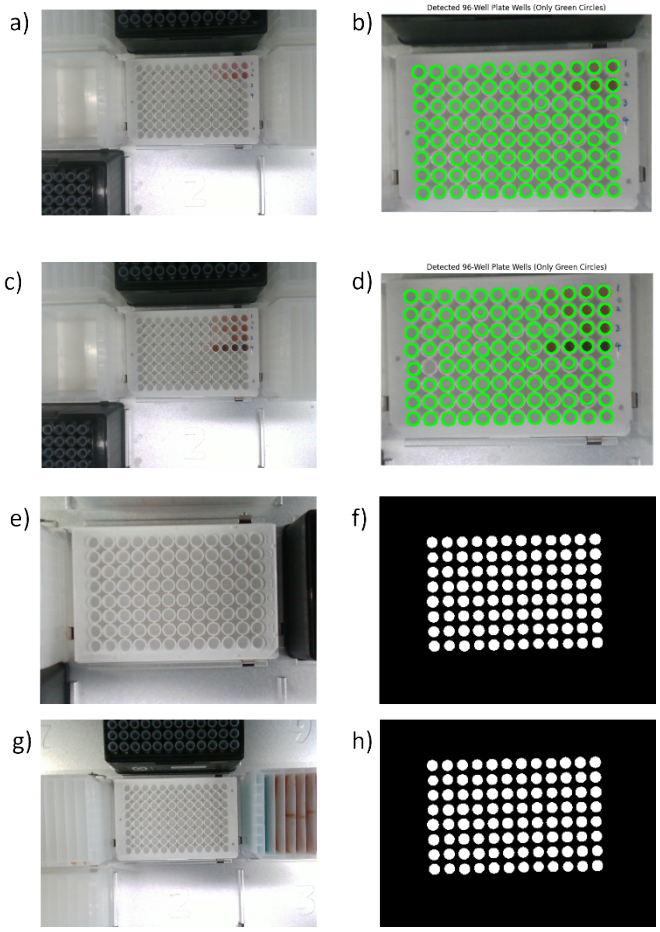

Figure S6 ((a) and (c) show images captured at different time points with the same camera-to-plate distance; (b) and (d) display the segmentation results using the Hough Circle Transform method; (e) and (g) illustrate images taken at varying camera-to-plate distances on our workstation; (f) and (h) present the corresponding segmentation results obtained using the VGG-augmented U-Net model.

Before protocol execution, we aligned the camera's field-of-view with respect to the 96-well plate and inspected imaging parameters such as frame rate (default: 1 fps), sensitivity, and total number of frames to be acquired. To align the camera, we manually moved OT-2 pipette mount while acquiring frames independently at a high frame rate, typically 30 fps. Deck 5 was our usual choice for placing a 96-well plate, and the optimal camera position for capturing deck 5 was equivalent to moving the P20 GEN2 pipette mounted on the right side of the pipette assembly to deck 3 well D3. To maintain consistency across different images while ensuring the well plate remained the primary focus, a simple cropping method with fixed paddings was chosen to preprocess images before extract colour information. Following this, a basic Hough Circle Transform method was applied to detect the wells and confirm the Region of Interest (ROI). However, as shown in Figure S6(a-d), despite maintaining the same camera-to-plate distance, the cropped images displayed instability in the plate view. Besides, some wells were missing, and the detected green circles varied slightly in position and size. These inconsistencies indicated that the current method lacked the robustness required for a stable and reproducible analysis pipeline within our workstation. To overcome these limitations and enhance detection accuracy and robustness, some deep learning-based approaches were considered. Instead of deploying computationally intensive instance segmentation models, such as MaskRCNN and YOLO[4,5], for extracting colour patches from wells, a relatively straightforward VGG-augmented UNet[6] was employed. The trained VGG-augmented UNet (test IOU > 0.95) predicted a binary mask capturing circular/elliptical well patches. This binary mask aided in locating bounding boxes circumscribing well contours. Utilizing these

boundary boxes directly for extracting colour patches may add significant noise to mean colour if the liquid does not consume the entire well volume; hence, 16% of the area of the bounding boxes was rejected. These bounding boxes were sorted using centre coordinates and mapped with appropriate well numbering; that is A1 to H12. Notably, as illustrated in Figure S6(e-h), VGG-augmented UNet demonstrated consistent and robust performance even when the camera-to-plate distance varied. This adaptability makes it particularly suitable for deployment on another OT-2 using the same camera.

Based on the colour change from transparent to pale pink, the CIELab colour model[7] was selected to analyse the image from those developed colour models, such RGB, CIE 1931, CIE XYZ, HSV, CIELab, *etc.* The CIELab colour model covers the entire gamut (range) of human colour perception and is divided into three matrices L*, a*, and b* as shown in Figure S7. The matrix of pixel values of parameter L* is for perceptual lightness, and a* and b* are for four unique colours of human vision: red, green, blue and yellow. The matrix of pixel values of parameter a* axis is relative to the green-red opponent colours, with negative values toward green and positive values toward red. The matrix of pixel values of parameter b* axis represents the blue-yellow opponents, with negative numbers toward blue and positive toward yellow.

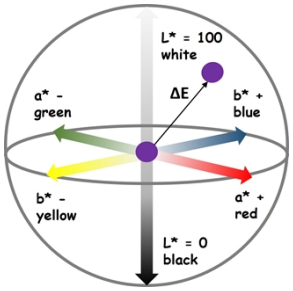

Figure S7 The CIELab[8] colour space diagram, defined by the International Commission on Illumination (abbreviated in CIE) in 1976.

5.2 Plate preparation/Pre-estimation image analysis

All our titration experiments used white-coloured 96 well plates to eliminate diffuse scattered light during imaging and minimize crosstalk between wells. The above image analysis method was utilized to analyse the images captured in plate preparation, pre-estimation, and titration, respectively.

For H_2O_2 determination, the a* value effectively quantifies colour changes in our colorimetric titration experiment, where the titration endpoint transitions from colourless to pale pink. The robot OT-2 combined with a webcam was utilized to develop an HTE H_2O_2 determination method based on chemical titration using the titrant $KMnO_4$.

Plate preparation:

For the image obtained after completing the plate preparation, the above-mentioned instance segmentation method was utilized, and the colour analysis area of each well was generated. Due to the same light environment condition used within one plate, the generated mask file (mask.pkl) was further used to analyse the images produced from pre-estimation and titration.

Pre-estimation:

The most important aim in this step was to confirm the titrant $KMnO_4$ concentration. Based on the experimental details described in section 2 protocol development, the aim could be further translated into finding the first well with a* >0, after adding 40 µL of $KMnO_4$ with a known concentration (1, 2, 4, and 10 mM). The logic details of the pre-estimation are shown in Figure S8.

5.3 Fitting analysis in titration

After obtaining the titrant $KMnO_4$ concentration from the pre-estimation, this titrant was further used to execute titration step to quantify the H_2O_2 concentration. In this part, 13 points were obtained for each sample and further a piecewise fitting was applied. Initially, linear (when a*<0) and a Tangent (when a*>0) basis functions were performed as shown in Figure S10(a, b). It showed a good fitting result when H_2O_2 concentration was below 4 mM,

but a* exhibited a decreasing trend when it came to the concentration range of 4 ~ 10 mM (Figure S10(c)), which caused a huge influence on extracting the titration endpoint (Figure S10(d)). This was because when a high $KMnO_4$ solution was used, the colour of this solution was not only purple but a bit darker in terms of light strength in the CIELab colour model. Thus, the a* of the titrated solution after reaching the equilibrium was affected by the darkness of the high concentration of $KMnO_4$ solution, even though it was still higher than 0 (a*>0). This could be further explained by the light strength has some correlations with the a*. To diminish this effect, deleting some points after showing a decreasing trend was adopted, but it still had a large difference when extracting the intersection as the titration endpoint (Figure S10(e)). Thus, a polynomial function fitting model was chosen to replace the current curve fitting in Figure S10(f). Its power was adjusted several times, and 4 mostly showed good accuracy when compared with the H_2O_2 concentration results obtained by the traditional iodometry method, a typical titration combined with a UV-Vis spectrometer. The relative difference was approximately 10 %. However, sometimes only 3 data points were obtained when H_2O_2 concentration approached the upper limit of a given range. Although one data point with a* < 0 was already included in the fitting process to better approximate the intersection, the number of data points remained insufficient for fourth-degree polynomial fitting, as shown in Figure S10(g). But due to titration design, a minimum of three data points was always ensured, enabling third-degree polynomial fitting as a viable alternative while also reducing operation time (Figure S10(h)). This was further elaborated in Figure S9.

After completing the signal processing and fitting analysis, the given volume will be put into the designed Excel to calculate H_2O_2 concentration as shown in Table S4.

Table S4 The designed Excel for the H_2O_2 concentration calculation

sample	Initial result	H_2O_2 Conc. (UV)	consumed $KMnO_4$ volume (OT-2)	$KMnO_4$ Conc.	H_2O_2 Conc. (OT-2)	Relative Difference	Absolute Difference (UV-(OT-2))
-	(a.u.)	(mM)	(μL)	(mM)	(mM)	(%)	(mM)
1	2.783	0.498	17.432	0.976	0.425	14.520	0.073
2	6.650	1.189	24.152	1.944	1.174	1.281	0.015
3	25.870	4.626	18.866	10.339	4.876	-5.420	-0.25
…	…	…	…	…	…	…	…

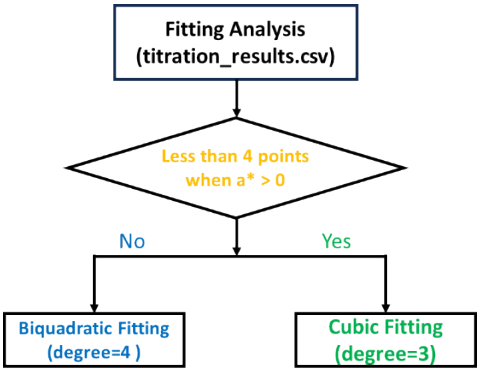

Figure S9 The process of third/fourth-degree polynomial fitting function selection.

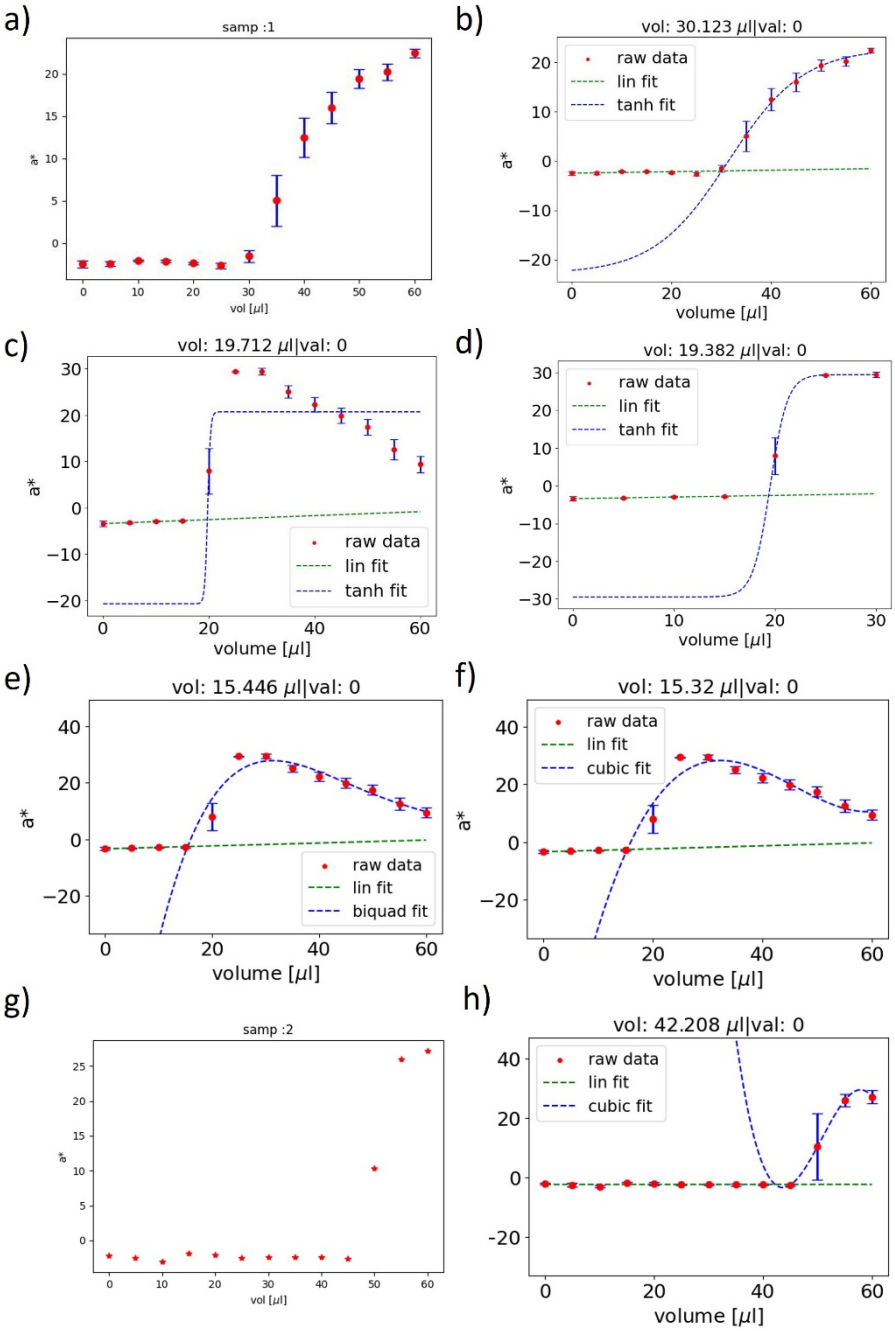

Figure S10 a) Scattering plot of the titration results for a sample.; b) Old piecewise fitting model using linear fitting and the Tanh basis function. c) - f) Scattering plots and fitting models for another sample: c) Old piecewise fitting using linear fitting and Tanh basic function; d) Improved fitting model with selected points removed from the decreasing interval; e) and f) New piecewise fitting model combining linear and polynomial fitting: biquadratic fitting and cubic fitting; g) -h) Scattering plots and fitting models for another sample with less than 5 points after a >0.*

6 The schematic diagram of this workstation

6.1 The schematic diagram of this workstation

To improve the clarity of running this workstation for new users, a schematic diagram was illustrated in Figure S11, which provide a step-by-step operation details for setting up and executing the experiments.

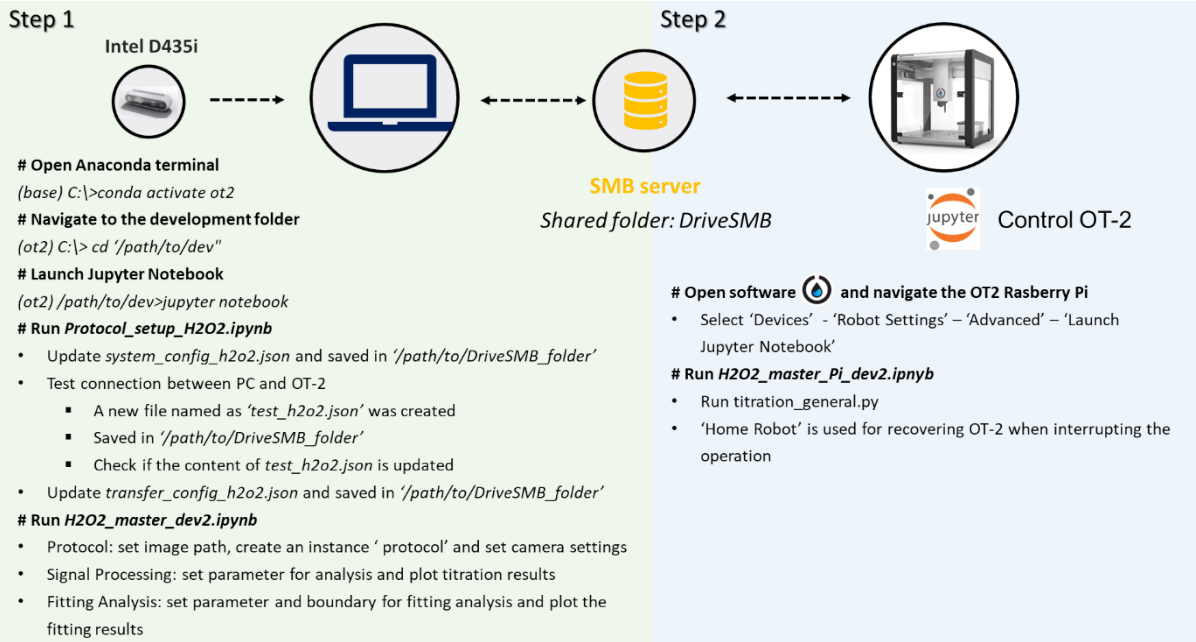

Figure S11 The schematic diagram of this workstation.

6.2 Software & Packages used in this workstation

Intel RealSense, Numpy,[9] Scipy,[10] Pandas,[11] Matplotlib,[12] Scikit-Learn,[13] PyTorch,[14] OpenCV,[15] Pysmb[16]

7 Evaluation

7.1 Sensitivity test

This part was used to relate the a* value of the CIELab colour model to the absorption value of the plate reader (Instrument type: Thermoscientific Varioskan Lux) based on UV-Vis spectroscopy, which could reflect the sensitivity of our automated H_2O_2 determination method.

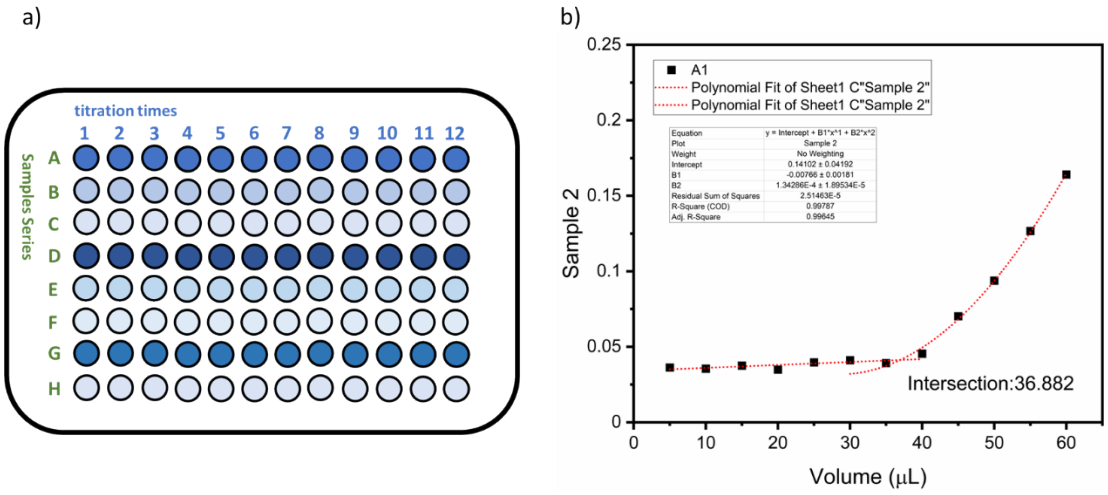

Figure S12 a) The illustration experimental layout used for the plate reader; b) The illustration fitting model used for the plate reader titration results.

Different from our automated H_2O_2 determination method, experiments carried out by the plate reader followed the row direction as shown in Figure S12(a). Each well in a row was charged with 100 µL 1M H_2SO_4, 100 µL H_2O_2, and

a certain amount of $KMnO_4$ (5 μL* ordinal number of well), which corresponds to the titration step with 12 times titration in our automated H_2O_2 determination method. The absorption value at the wavelength of 525 nm was selected to gain the titration endpoint for the plate reader. For this fitting, similarly, a linear fitting and a polynomial function (power = 2) fitting model were chosen as shown in Figure S12(b). These H_2O_2 solutions were measured again using our automated H_2O_2 determination method. After gaining the consumed volume of $KMnO_4$ solution, these values were put into Table S5 to calculate H_2O_2 concentration and summarized in Table S6.

Table S5 The summarized data for the sensitivity test

Location	$KMnO_4$ Conc. mM	Consumed $KMnO_4$ volume (PR) μL	Consumed $KMnO_4$ volume (OT-2) μL	H_2O_2 Conc. (PR) mM	H_2O_2 Conc. (OT-2) mM
A1	1.018	25.145	24.422	0.640	0.622
A2	2.091	29.943	27.063	1.565	1.415
A3	4.126	33.203	29.001	3.425	2.991
A2	2.091	35.844	32.037	1.874	1.675
A3	4.126	22.602	18.914	2.331	1.951
A1	1.018	15.557	13.591	0.396	0.346
A1	1.018	23.118	22.058	0.588	0.561
A4	10.390	41.903	39.208	10.884	10.184
A4	10.390	21.241	19.819	5.517	5.148
A3	4.126	34.678	31.155	3.577	3.214
A3	4.126	20.525	18.974	2.117	1.957
A2	2.091	20.538	19.490	1.074	1.019
A2	2.091	24.006	22.376	1.255	1.170
A2	2.091	22.600	21.680	1.181	1.133
A3	4.126	23.930	21.404	2.468	2.208
A1	1.018	8.514	8.100	0.217	0.206
A1	1.018	36.882	33.795	0.939	0.860
A2	2.091	36.853	32.775	1.926	1.713
A3	4.126	42.622	38.116	4.396	3.932
A2	2.091	44.559	40.102	2.329	2.096
A3	4.126	26.232	23.486	2.706	2.423
A1	1.018	22.173	18.896	0.564	0.481
A4	10.390	35.058	31.869	9.106	8.278
A4	10.390	32.063	30.009	8.328	7.795
A4	10.390	26.272	26.427	6.824	6.864
A4	10.390	25.414	22.700	6.601	5.896
A4	10.390	25.771	24.152	6.694	6.273
A4	10.390	26.042	24.608	6.764	6.392
A4	10.390	26.247	25.119	6.817	6.524
A4	10.390	29.592	26.217	7.686	6.810

*A1-A4: location of $KMnO_4$ in the $KMnO_4$ reservoir; PR: plate reader; OT-2: Opentrons.

We also explore the influence of the different types of plate on the colour change observed by the camera installed on the pipette mount of OT-2 as shown in Figure S13. The white plate could sharpen the colour change when it closed to the titration endpoint. It is noteworthy that the transparent plate was only for the illustration of phenomenon comparison when using different colours of the plate, not the real experiment.

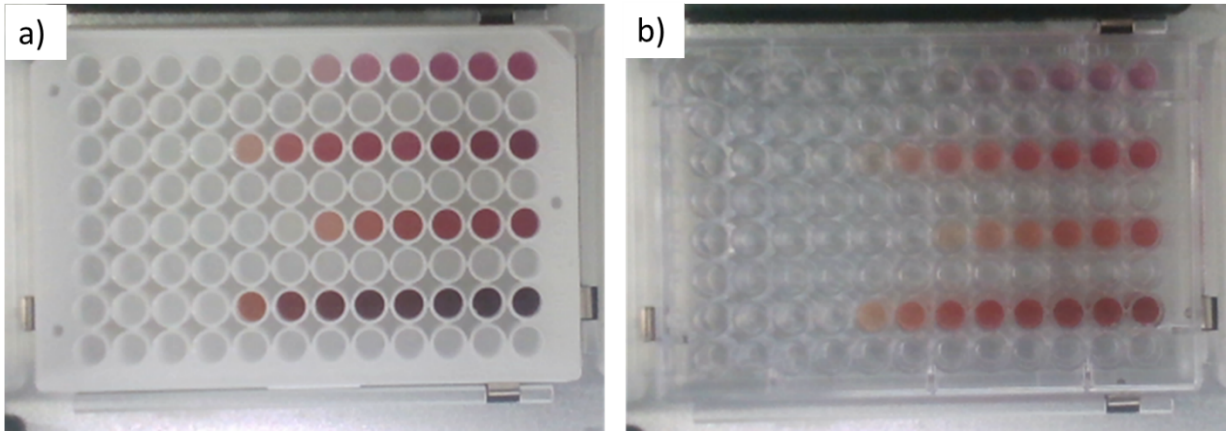

Figure S13 The comparison of white/transparent 96-well plate.

To further verify this difference, the type of plate was set as the only variable for the control experiment, and its result was summarised in Figure S14. In most cases, the consumed volume of $KMnO_4$ from the white plate was lower than the transparent plate. With the increase in H_2O_2 concentration, the volume difference became smaller. In addition, the error bar when using a white 96-well plate was lower than that when using the transparent 96-well plate, which also verified that the selection of the white 96-well plate could improve the sensitivity of the CIELab colour model.

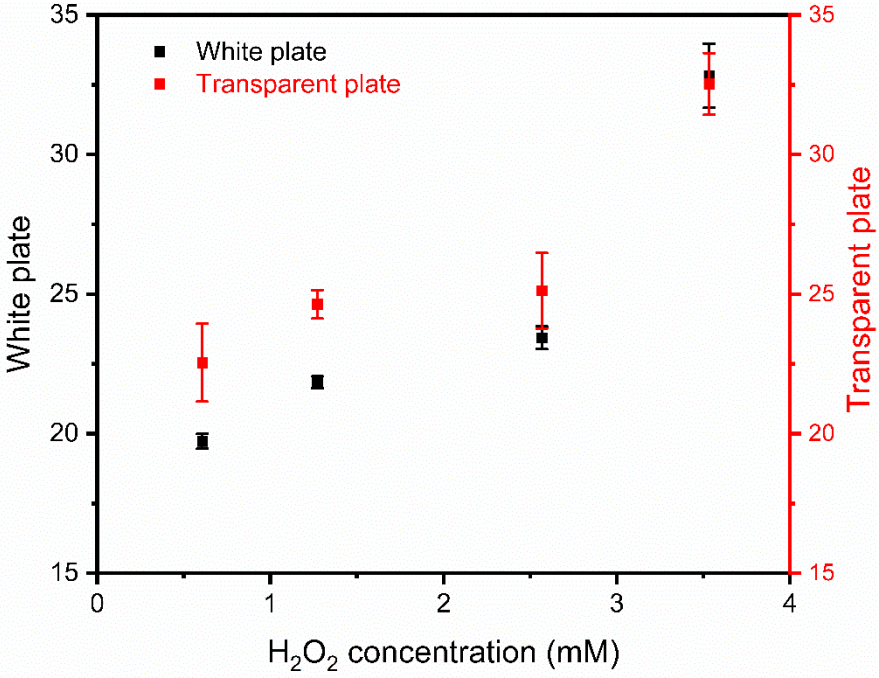

Figure S14 The comparison of estimated H_2O_2 concentration when using a 96-well plate of different colours (x – H_2O_2 concentration, y- consumed volume of $KMnO_4$).

7.2 Precision test

In this experiment, four unknown samples were measured, and each sample was measured three times. Besides, the significant figure was also considered when evaluating the obtained volume. Two types of pipettes, multi-channel P300 GEN2 pipette (volume range: 20-300 µL) and single-channel P20 GEN2 pipette (volume range: 1-20 µL), were used. Among them, the working limit was dependent on the low volume of the single-channel P20 pipette, and its working limit was 1 µL, which was used for the significant figure evaluation of precision test.

7.3 Linear dynamic range

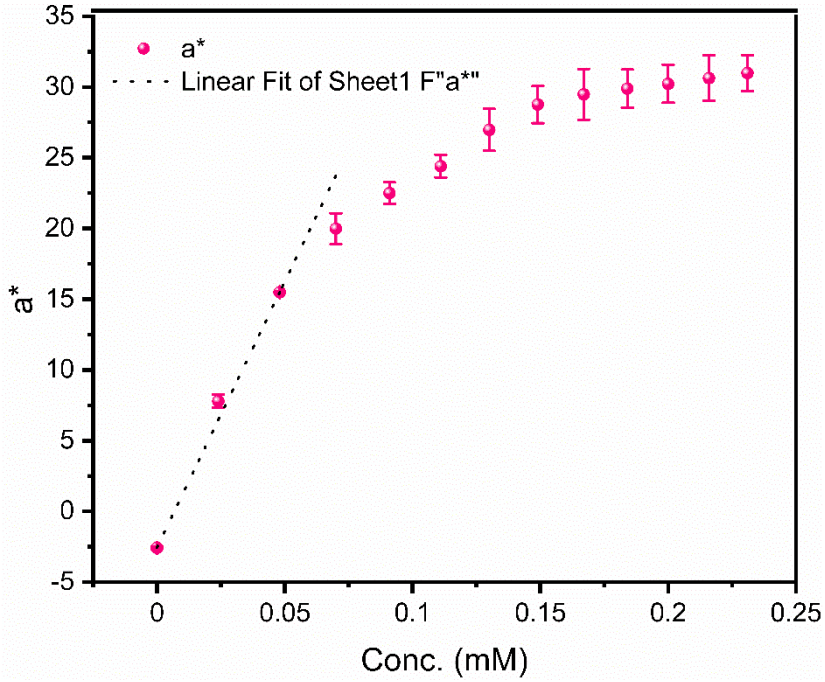

Figure S15 The linear dynamic range of the high-throughput H_2O_2 determination using an automated pipetting robot OT-2.

In this experiment, the 100 µL H_2O_2 was replaced by water and 1 mM $KMnO_4$ was utilized as the titrate. The colour change was recorded by the webcam and analysed by applying CIELab colour model as exhibited in Figure S15.

7.4 Accuracy test

For the accuracy test, the frequently used in the reported literature, the iodometry method[1,17] was selected as the method of obtaining true value. In the iodometry method, the amount of H_2O_2 production was carried out by UV-vis spectroscopy and its mechanism is as follows:

$$_3I^- + H_2O_2 + 2H^+ = I_3^- + 2H_2O$$

1 mL 0.1 M $C_8H_5KO_4$ and 0.4 M KI were separately added to the semi-micro cuvette. To determine the concentration of H_2O_2, a 0.2 µm Millipore filter first filtered the reaction solution to remove the photocatalyst and then 0.5 mL of it was added to the semi-micro cuvette. After 30 minutes, the product (I_3^-) which possesses an absorption at 350 nm was measured by UV-Vis spectrometer and its standard calibration curve was illustrated in Figure S16. In addition, the standard calibration curve of $KMnO_4$ was illustrated in Figure S17.

All the original data used to evaluate the accuracy of the developed HTE H_2O_2 robotic determination method is stored in in the directory /Data/Demo/H_2O_2, accessible at https://doi.org/10.5281/zenodo.149895187.

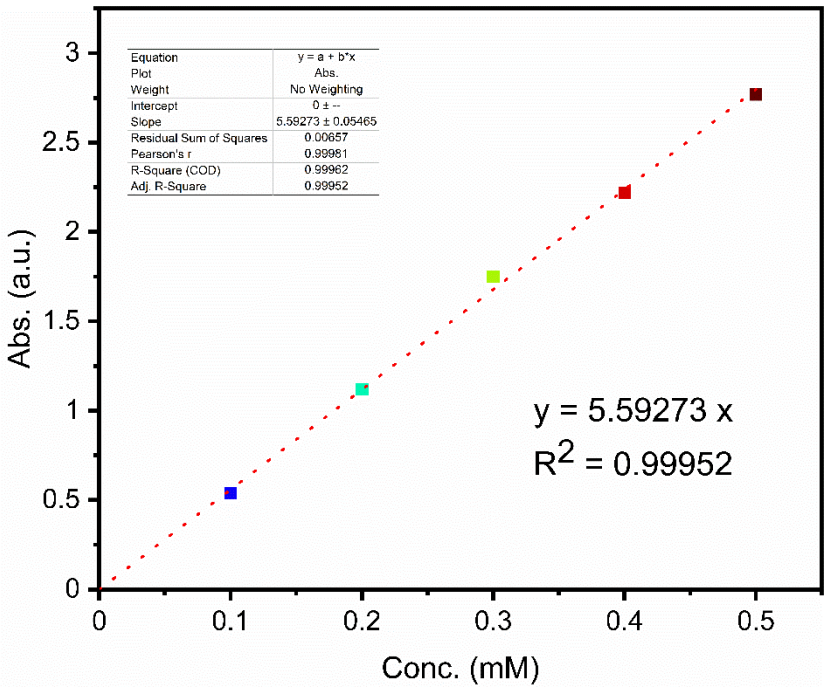

Figure S16 The calibration curve of the iodometry method.

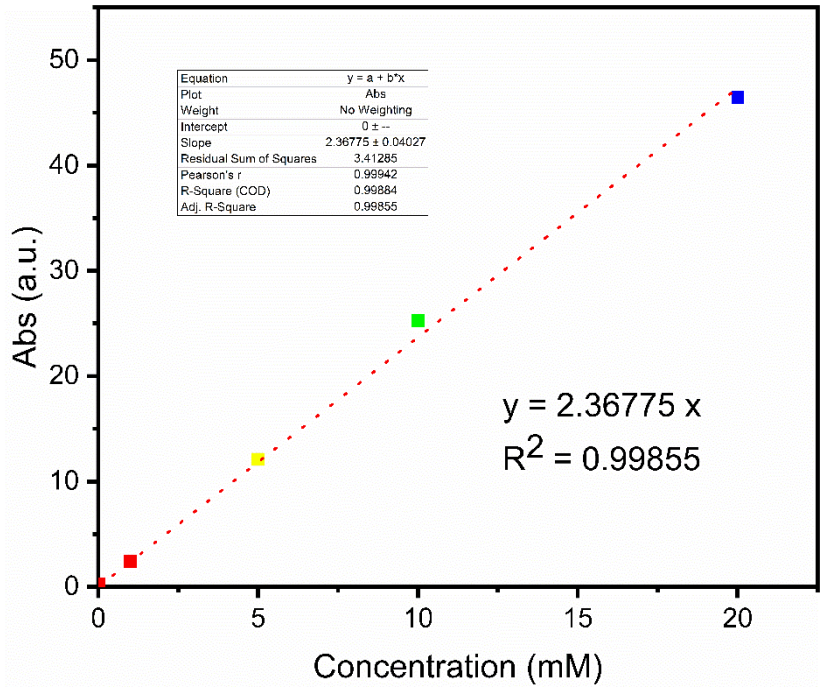

Figure S17 The calibration curve of $KMnO_4$ solution.

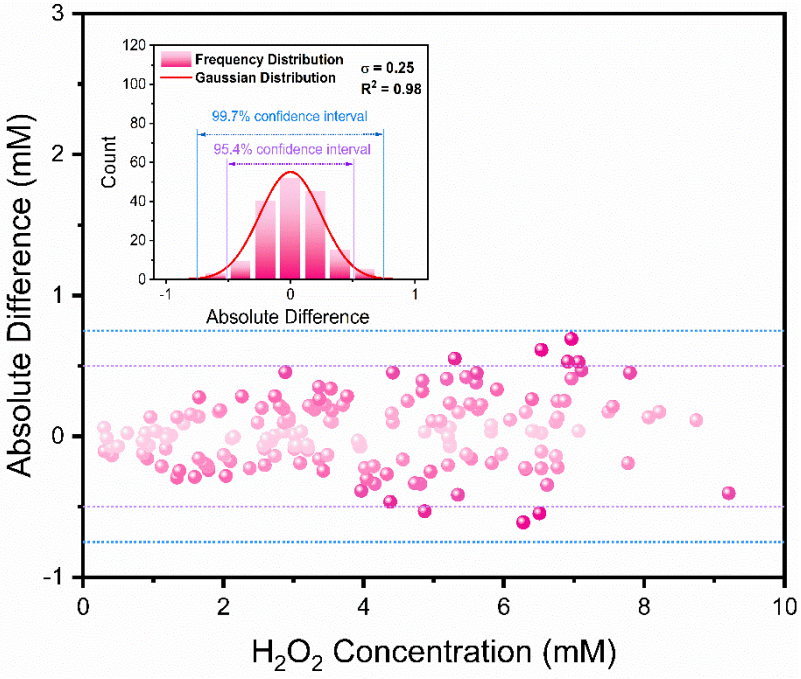

Figure S18 The relationship between the absolute concentration difference and H_2O_2 concentration (The lighter of the pink dot is, the closer the absolute difference is closer to zero). The inset plot is the frequency distribution of the absolute difference (bin range: ±1, bin width: 0.2) and its Gaussian distribution (X_c = 0, y_0 = 0) as shown in the red line

Table S6 The calculation details of the accuracy test.

sample	Initial result	H_2O_2 Conc. (UV-Vis)	consumed $KMnO_4$ volume (OT-2)	$KMnO_4$ Conc.	H_2O_2 Conc. (OT-2)	Relative Difference	Absolute Difference (UV-OT-2)
	a.u.	mM	μL	mM	mM	%	mM
1	2.783	0.498	17.432	0.976	0.425	14.520	-0.072
2	1.901	0.340	13.429	0.976	0.328	3.597	-0.012
3	5.271	0.942	18.506	1.894	0.876	7.036	-0.066
4	6.589	1.178	23.024	1.894	1.090	7.465	-0.088
5	7.690	1.375	23.858	1.894	1.130	17.851	-0.245
…	…	…	…	…	…	…	…
203	34.788	6.220	24.098	10.390	6.259	-0.628	0.310
204	31.223	5.583	20.093	10.390	5.219	6.515	-0.121

7.5 The operation time

For evaluating the operation time, the stability of the $KMnO_4$ solution was also measured by a UV-Vis spectrometer. As shown in Figure S19, the $KMnO_4$ concentration kept intact within 6 h.

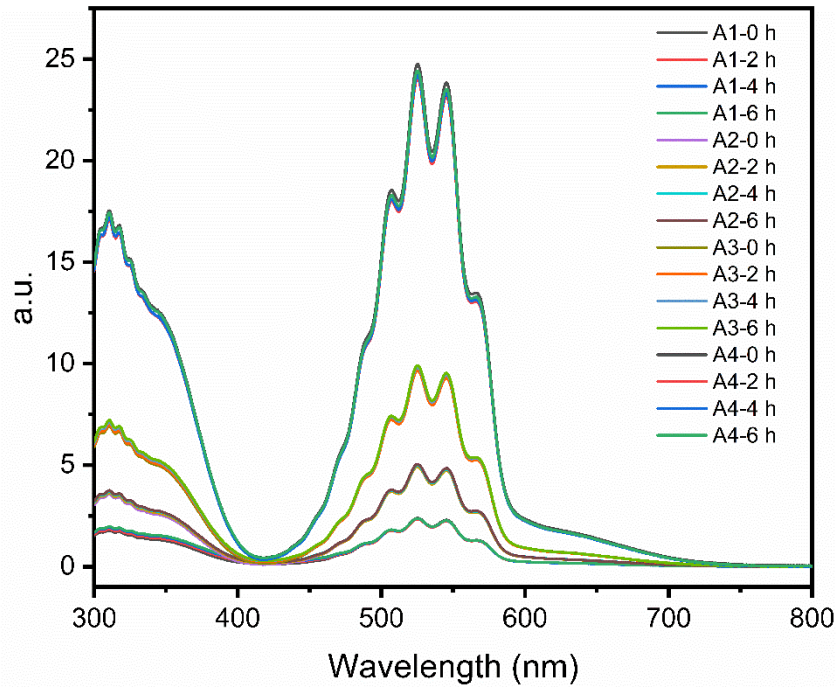

Figure S19 The stability test of $KMnO_4$ solution in 6h.

7.6 The scalability test

For evaluating the flexibility of this analytical method, a 24-well white plate was chosen to explore the impact of the plate dimensions and number of wells on reaction colour monitoring.

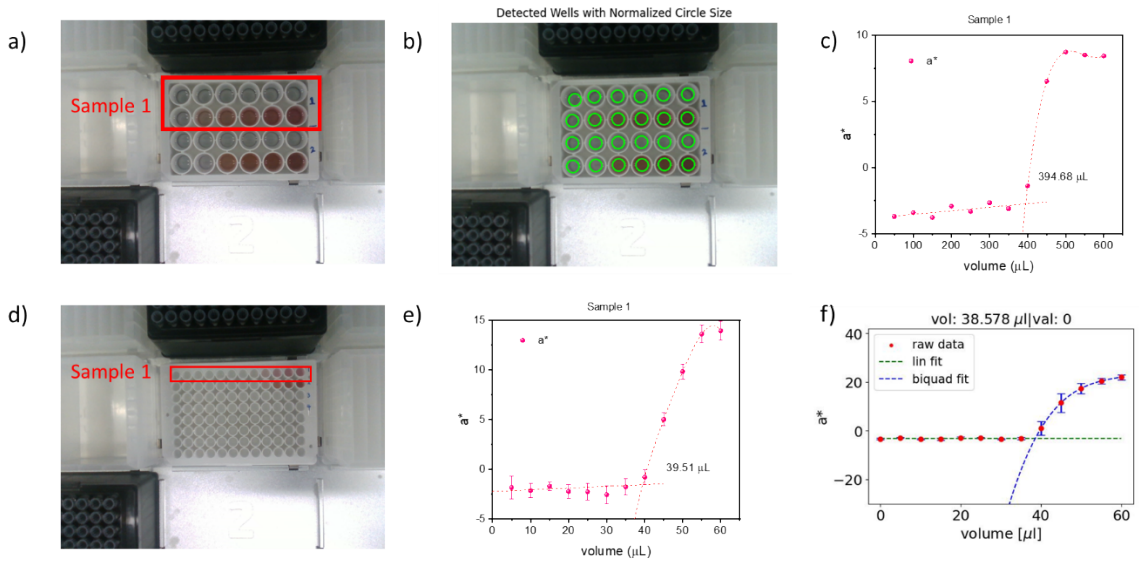

Figure S20 The scalability test.

In this experiment, solutions of $KMnO_4$, H_2O_2, and H_2SO_4 were prepared at the same concentration and tested in both 24-well and 96-well white plates. The reaction volume in the 24-well plate was 10 times larger than that in the 96-well plate. Because these experiments are quite different from the process of our designed workflow. Firstly, t All experiments and images were taken by the camera in our designed workstation, but it is just used Opentrons protocol designer. For the 24-well plate (Figure S20), its result was analysed by a simple Hough Circle transform, which

provides the center coordinates (x, y) and the radius of each circle (details could be found in the directory Data/Demo/scalability_test, accessible at https://doi.org/10.5281/zenodo.149895187). Then, a circular mask was created and used to extract region of interest (ROI) information. The average colour of each well was calculated and the consumed $KMnO_4$ volume was 394.68 μL in Figure S19(c). Compared with the complex VGG-augmented UNet method, this simple method could achieve fast analysis though the precision is a bit lower. As shown in Figure S20(d), column 1 -12 showed each step of the titration result carried out in our workstation and its result was carried out by VGG-augmented UNet method.

8 Application

8.1 Monitoring H_2O_2 production through photocatalysis

8.1.1 The synthesis of DE7

Synthesis of DE7[18]: A 40 mL glass vial was charged with 2,5-Dibromopyridine (237 mg, 1 mmol), 1,4-diethynylbenzene (126 mg, 1 mmol), $Pd(PPh_3)_2Cl_2$ (18 mg, 0.025 mmol), CuI (2 mg, 0.010 mmol), triphenylphosphine (13 mg, 0.050 mmol), N,N-dimethylformamide (9 mL) and triethylamine (9 mL), and then sealed with a silicone septum in a glove box. The sealed vessel was taken out of the glove box, placed in a microwave chamber, and then heated to 80 °C for 2 h. After the reaction was cooled to room temperature, the mixture was quenched by adding methanol. The resulting solids were then filtered and washed with methanol and acetone orderly. Further purification was carried out by Soxhlet extraction with chloroform for 2 days. The final product was dried in the vacuum oven at 80 °C overnight. The final product was obtained as a yellow solid. (193 mg, 96%).
Anal. Calca. for $(C_{15}H_7N)n$: C, 89.53%; H, 3.51%; N, 6.96%. Found: C, 76.33%; H, 3.28%; N, 5.42%. Pd content: 0.27%, Cu content: 0.02%. These values are consistent with the reported values in the literature[17,18].

8.1.2 The reaction conditions for H_2O_2 photoproduction using DE7

In this experiment, a flask was charged with 30 mL water and 50 mg DE7 and sealed with a rubber septum. The suspension was ultrasonicated for 10 min to disperse well before degassing by O_2 for 10 min. The reaction solution was illuminated by a 300 W Xe lamp with a filter ($\lambda > 420$ nm) and kept at room temperature by air cooling. 1 mL solution was sampled with an injection syringe after being shaken evenly and then filtered with a 0.2 μm Millipore filter to remove the photocatalyst every hour. Then, the H_2O_2 concentration was measured by our developed high-throughput H_2O_2 determination using an automated pipetting robot. Simultaneously, the concentration of H_2O_2 was determined using the iodometry method as a reference.

8.2 Parameter Selection

To highlight the modularity feature of our designed workstation, we first evaluated which colour parameter is capable to distinguish different colours as the concentration changes.

As shown in Figure S21(a), different concentrations of various colours were prepared in a 96-well plate, and their L, a*, and b* values were obtained using our independent image_analysis.py script. Figure S21(b-d) illustrate the variations of L, a*, and b* across different wells. However, none of these parameters exhibited a consistent trend for a single colour. The L parameter tended to converge as the colour concentration decreased. For a* and b*, their ability to distinguish colours diminished when the colour was either too dark or too light, and some colours exhibited a curved trend, which could significantly impact colour measurement accuracy. To address this issue, we selected the CIELCh colour model, which directly derives its scale values from the CIELab model. As shown in Figure S21(e), the L parameter represents lightness, consistent with the CIELab scale. The C parameter represents chroma, while the h parameter, the hue angle, is calculated from the a* and b* values of the CIELab scale. Within the green area of the Figure S21(f), different colours exhibit distinct hue values, but these values are less affected by concentration. This observation aligns with the CIELCh 3D colour space shown in Figure S21(e). This stability makes hue a useful parameter for evaluating reactions that involve colour changes. Thus, acid-base titration using pH indicator and

complexometric titration (Ca^{2+} analysis using EDTA) were chosen to evaluate the universality of our workstation. Due to the change of the parameter used in signal processing, three parameter - *params*, *boundary*, and *larger_than_boundary* - were introduced to support pre-estimation and fitting analysis after titration, which highly improve the flexibility of this workflow.

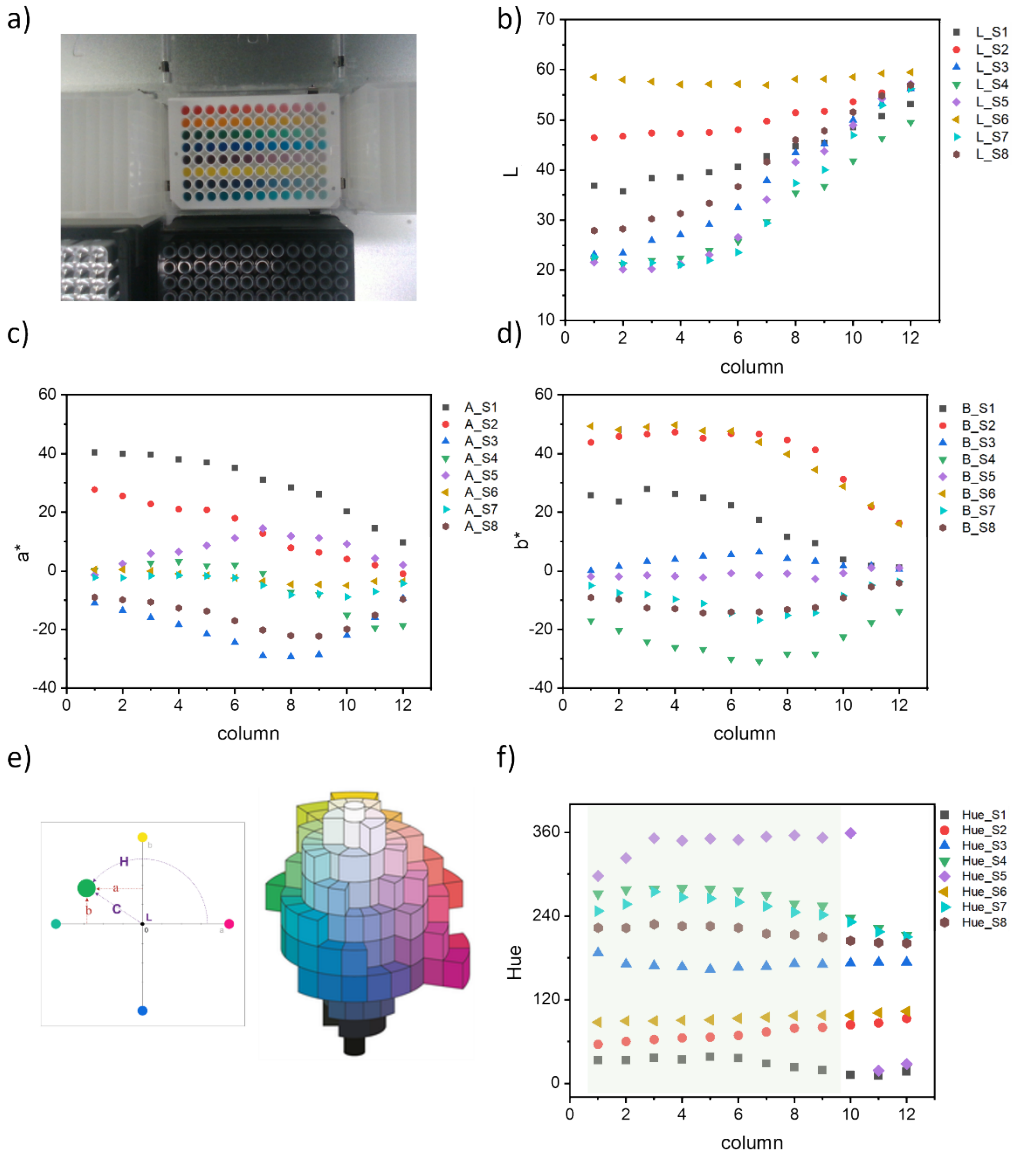

Figure S21 (a) Image captured from our workstation: Each row of the 96-well plate contains a different colour, while the concentration decreases from left to right. Each column maintains the same concentration; (b-d) Scattering plot of L, a, and b* parameter across different wells; (e) Illustration of the calculation of CIELCh colour model from CIElab colour model and its 3D colour space representation (Image source: "CIELAB colour space, Cylindrical model" Wikipedia, The Free Encyclopaedia. Available under the CC BY-SA 4.0 license); (f) Scattering plot of h parameter across different wells.*

8.3 The acidity/alkalinity test

Like H_2O_2 determination, the process consists of three steps: plate preparation (addition of methylene orange and hydrochloric acid), pre-estimation, and titration. For acidity/alkalinity test, we selected hydrochloric acid as the sample, methyl orange as the pH indicator, and sodium hydroxide as the titrant. However, the titration endpoint of pH indicator is determined by the turning point of the selected indicator rather than the stoichiometric equivalence of acid and base. For example, methyl orange changes colour within a pH range of 3.1-4.4. During titration, the colour of the solution changes from red to orange and then to yellow, corresponding to a hue shift from ~30 to ~60 as shown

in Figure S22. Thus, the *boundary* used in the pre-estimation was set as 50. Each volume step and times of titration were set as 4 μL and 15. The concentrations and volumes of hydrochloric acid, methyl orange, and sodium hydroxide, along with calculation details for pre-estimation and fitting analysis of titration, are available in in the directory Data/Demo/pH folder, accessible at https://doi.org/10.5281/zenodo.149895187.

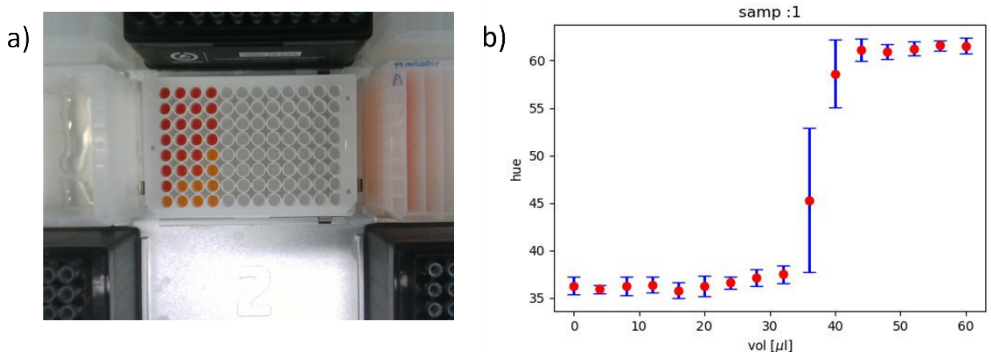

Figure S22 (a) The pre-estimation result of an example for the acidity test; (b)The titration results of the acidity test.

8.4 Water hardness analysis (Calcium Analysis by EDTA titration)

Preparation of 0.025 M EDTA original solution:

Using the top loading balance, weigh 0.4653 g of disodium EDTA dihydrate into a clean 50 mL centrifuge tubes. (EDTA will leach metal ions from soft glass containers and should never be stored in glass containers.) Add 50 mL of deionized water. EDTA dissolves slowly. Shaking or stirring the solution vigorously speeds the dissolution process. Use the analytical balance, weigh out 13 mg Magnesium chloride **(**$MgCl_2$) and add it to the EDTA solution.

Preparation of Ca^{2+} solution:

Dry about 1 gram of calcium carbonate ($CaCO_3$) in the oven for 2 hours at 60 °C. Transfer to the desiccator and cool. When cooled, weigh 0.5 g $CaCO_3$ on the analytical balance and transfer it to a clean 250 mL beaker. Add approximately 25 mL of distilled H_2O, then 5mL of concentrated hydrochloric acid carefully to the 250 mL beaker. When the calcium carbonate has completely dissolved, boil the solution gently for 2-5 minutes to expel carbon dioxide. Analytically transfer the solution to a 500 mL volumetric flask and dilute with DI water. Check the pH using pH paper: If acidic, use dilute sodium hydroxide solution to adjust the pH to ~7.

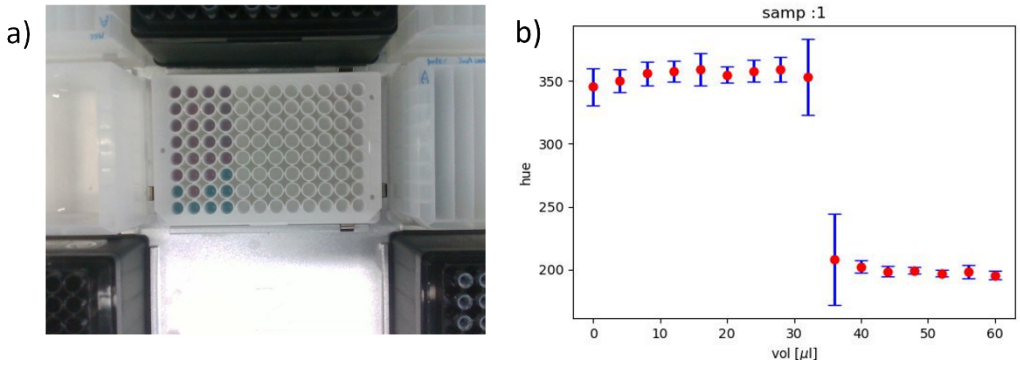

Figure S23 (a) The pre-estimation result of an example for calcium analysis; (b)The titration results of the calcium analysis.

For water hardness analysis, we selected Ca^{2+} solution as the sample, Eriochrome Black T (EBT) as the indicator, ammonium buffer (pH=10) solution as the buffer and EDTA solution as the titrant. Like H_2O_2 determination, the process consists of three steps: plate preparation (addition of buffer, indicator and sample), pre-estimation, and titration. The titration endpoint in this process is determined by the stoichiometric equivalence of EDTA and Ca^{2+}. Initially, EBT forms a stable wine-red complex ($MgIn^-$) with the Mg^{2+}. A tiny amount of this complex will be present

in the solution during the titration. As EDTA is added, it complexes with free Ca^{2+} and Mg^{2+} ions, leaving the $MgIn^-$ complex intact until essentially all the Ca^{2+} and Mg^{2+} has been converted to chelates. At this stage, the EDTA concentration will increase sufficiently to displace Mg^{2+} from the indicator complex, causing EBT revert to its acid form (sky blue), which means that the titration endpoint has been reached. During titration, the solution colour transitions from wine-red to sky blue, corresponding to a hue shift from ~350 to ~200 (Figure S23). Thus, the *boundary* used in the pre-estimation was set as 220. Each volume step and times of titration were set as 4 μL and 15. The concentrations and volumes of Ca^{2+} solution, EBT, ammonium buffer (pH=10) solution and EDTA solution, along with calculation details for pre-estimation and fitting analysis of titration, are available in available in the directory Data/Demo/wha (https://doi.org/10.5281/zenodo.149895187).

References

1 L. Wang, J. Zhang, Y. Zhang, H. Yu, Y. Qu and J. Yu, *Small*, 2022, **18**, 2104561.

2 T. Liu, Z. Pan, J. J. M. Vequizo, K. Kato, B. Wu, A. Yamakata, K. Katayama, B. Chen, C. Chu and K. Domen, *Nat. Commun. 2022 131*, 2022, **13**, 1–8.

3 K. Thurow and S. Junginger, *Devices and Systems for Laboratory Automation YR - 2023*, John Wiley & Sons, 2023.

4 K. He, G. Gkioxari, P. Dollár and R. Girshick, *arXiv:1703.06870*.

5 J. R. Terven and D. M. Cordova-Esparza, *arXiv:2304.00501v7*.

6 V. Iglovikov and A. Shvets, *arXiv:1801.05746*.

7 N. Phuangsaijai, J. Jakmunee and S. Kittiwachana, *J. Anal. Sci. Technol.*, 2021, **12**, 1–16.

8 L. F. Capitán-Vallvey, N. López-Ruiz, A. Martínez-Olmos, M. M. Erenas and A. J. Palma, *Anal. Chim. Acta*, 2015, **899**, 23–56.

9 C. R. Harris, K. J. Millman and S. J. van der Walt, *Nature*, 2020, **585**, 357–362.

10 P. Virtanen, R. Gommers, T. E. Oliphant and S. 1. . Contributors, *Nat. Methods*, 2020, **17**, 261–272.

11 McKinney, in *Proceedings of the 9th Python in Science Conference*, 2010, pp. 56–61.

12 J. D. Hunter, *Comput. Sci. Eng.*, 2007, **9**, 90–95.

13 A. Pedregosa, F., Varoquaux, G., Gramfort, *J. Mach. Learn. Res.*, 2011, **12**, 2825--2830.

14 A. Paszke, S. Gross and F. Massa, in *Advances in Neural Information Processing Systems 32*, Curran Associates, Inc., 2019, pp. 8024–8035.

15 G. Bradski, *The Opencv Library*, 2000, vol. 25.

16 M. Teo, 2023.

17 L. Liu, M. Y. Gao, H. Yang, X. Wang, X. Li and A. I. Cooper, *J. Am. Chem. Soc.*, 2021, **143**, 19287–19293.

18 L. Liu, M. A. Kochman, Y. Xu, M. A. Zwijnenburg, A. I. Cooper and R. S. Sprick, *J. Mater. Chem. A*, 2021, **9**, 17242–17248.